

Tensile Properties Of *Attacus atlas* Silk Submerged in Liquid Media

J. PÉREZ-RIGUEIRO,¹ M. ELICES,¹ J. LLORCA,¹ C. VINEY²

¹ Departamento de Ciencia de Materiales, Universidad Politécnica de Madrid, ETS de Ingenieros de Caminos, Ciudad Universitaria, 28040 Madrid, Spain

² Department of Chemistry, Heriot-Watt University, Edinburgh EH14 4AS, Scotland

Received 7 August 2000; revised 30 October 2000; accepted 11 November 2000

ABSTRACT: Tensile properties of *Attacus atlas* (*Saturniidae*) silk were measured in air, water, and ethanol. Control samples in air showed a large variability, so a normalization method was developed to enable comparison with the behavior of samples submerged in the liquid media. Amino acid analysis demonstrated that the composition of *A. atlas* silk is similar to that of silk produced by other members of the *Saturniidae* family. The tensile properties of *A. atlas* silk resemble those of *Bombyx mori* (common domesticated silkworm) silk, although the two silks have different compositions. In particular, the elastic modulus is decreased by immersion in water and increased slightly by immersion in ethanol. The behavior of *A. atlas* silk can be described in terms of water having a disruptive effect on protein—protein hydrogen bonds, whereas ethanol acts as a desiccant and therefore enhances protein—protein hydrogen bonding. There are significant differences between the tensile properties of *A. atlas* silk and spider (*Nephila madagascarensis*) drag line, even though these materials have similar amino acid compositions: the spider silk has previously been shown to exhibit a decreased elastic modulus and conspicuous supercontraction in both liquids. Primary composition is therefore not a simple indicator of mechanical function in silks. © 2001 John Wiley & Sons, Inc. *J Appl Polym Sci* 82: 53–62, 2001

INTRODUCTION

Silk is a term used to describe the fibers that are spun from a protein solution by Arthropods (especially spiders and lepidopteran larvae). All silks exhibit combinations of tensile properties that rival or exceed those of artificial fibers;^{1, 2} however, each species produces fiber that has been optimized for its own purposes. If we are to derive broad biomimetic principles from these materials, it is necessary to establish relation-

ships between composition, microstructure, and mechanical properties in silks from different species. The number of silks studied thus far from a materials engineering point of view equates to a tiny fraction of the total available in nature: there are >30,000 species of spiders, each of which produces several types of silk, but only a few have been characterized in any detail.^{3, 4} Data from lepidopteran silks are similarly scarce, even though these materials outnumber the spider silks: only a limited number of species belonging to three families (*Bombycidae*, *Saturniidae*, and *Thaumetopoeidae*) have been studied.

The amino acid composition of silk can be determined by straightforward techniques.^{5–7} In all cases, glycine and alanine represent >50% of the

Correspondence to: J. Pérez-Rigueiro (jperez@mater.upm.es).

Journal of Applied Polymer Science, Vol. 82, 53–62 (2001)
© 2001 John Wiley & Sons, Inc.

total number of amino acids, although large differences have been found in the relative frequency of each amino acid. These differences were used by Lucas et al.⁵ to establish a first classification of silks. The classification parameter is $100 \times LC/SC$, where SC denotes a short-chain amino acid (Gly, Ala, Ser, and Thr) and LC denotes a long-chain amino acid (all others). The idea behind this classification is that SC amino acids would appear mainly in crystalline regions, whereas LC amino acids would concentrate in amorphous regions. We shall therefore refer to the classification parameter as the *disorder ratio* because a low content of SC (crystal building) amino acids is associated with a high value of the parameter.

The classification in terms of disorder ratio was restricted to moth larvae of the families *Bombycidae* (*Bombyx mori*), *Saturniidae* (*Antheraea mylitta* and *A. pernyi*), and *Thaumetopoeidae* (*Anaphe moloneyi*, *A. venata* and *A. infracta*) and one spider species (drag line from *Nephila madagascarensis*). It was found that the *Saturniidae* family achieves a disorder ratio of 27%. Interestingly, this value is the same as that found for *N. madagascarensis* silk. On the other hand, *Thaumetopoeidae* representatives yielded a much lower value of 5% and *B. mori* silk gave an intermediate value (13%). This classification can be expanded with data from other spider silks, presented in refs. 6 and 7, yielding values that lie between 25 and 40%. Another representative of the *Nephila* genus (*N. clavipes*) achieves a value of 25%, which is very close to the value for *N. madagascarensis* and the *Saturniidae*. These data indicate that each group produces silk of a characteristic composition, but different groups may also produce silk with similar composition, even if, like *Saturniidae* moths and *Nephila* spiders, they are distant in evolutionary terms.

Although it has become relatively easy to determine the amino acid composition and even the amino acid sequence for a protein, the characterization of microstructure at all relevant length scales continues to present a significant challenge. For this reason, information about silk microstructure has been obtained in only a few cases. Beta-sheet microcrystallites embedded in an amorphous matrix occur in *B. mori* silk,⁸ whereas major ampullate silk (the principal fiber in drag line) from *N. clavipes* spiders shows a more complex and hierarchical distribution of microcrystallites within the matrix.⁹

The difficulty of correlating composition and microstructure has prompted some attempts to correlate composition with mechanical properties directly. The underlying assumption is that similar compositions should give rise to similar microstructures, with the further assumption that processing conditions are also similar. Lucas et al.⁵ found that *Saturniidae* and *N. madagascarensis* silk showed lower values of the elastic modulus and larger extensibility when compared with the representatives of the *Thaumetopoeidae*. This fact correlates well with composition because the disorder ratio is larger for *Saturniidae* silk, indicating the presence of a lower crystalline fraction. A reduced crystalline fraction is likely to lead to a more compliant material, and the larger amorphous fraction explains the increase in extensibility. Finally, *B. mori* silk, whose disorder ratio lies between those of *Saturniidae* and *Thaumetopoeidae*, also shows intermediate mechanical properties (i.e., elastic modulus larger than for *Saturniidae* but lower than for *Thaumetopoeidae*).

The correlations between composition and mechanical properties just presented were established only from tensile tests in air. It would be instructive to also study samples tested under different environmental conditions to establish whether the correlations have wider validity. Moreover, a significant difference between spider drag line and *B. mori* silk appears when both materials are submerged in water. Spider drag line swells radially and contracts to $\sim 50\%$ of its original length (supercontraction), and its mechanical properties when wet become those of an elastomer.^{10–12} *B. mori* silk does not supercontract,⁴ but immersion in water again leads to a larger compliance.¹³ However, *B. mori* silk and the studied spider silks show different compositions as assessed in terms of their disorder ratio. It would therefore be appropriate to consider the mechanical properties of silk from a *Saturniidae* representative that achieves a similar disorder ratio to the spider silk. Consequently, the aim of the present work was to characterize *Attacus atlas* (*Saturniidae*) silk by performing tensile tests in air, water, and ethanol.

Our goal here (as well as in our previous and continuing studies) is to contribute to a comprehensive view of how silk composition, microstructure, and properties are interrelated. Ultimately, this information will be useful in the development of protein-based fibers that exhibit tailored combinations of properties in specified environments. At all length scales in the complex hierarchical

structure of silk, stability depends on a combination of covalent bonds, hydrogen bonds, and van der Waals bonds, and each of these classes of bond exhibits different environmental sensitivities.

EXPERIMENTAL

A. atlas silk was obtained from cocoons after a degumming treatment. The as-received cocoons had been wrapped by a leaf, which was cut and removed prior to starting the degumming process. Following the experience obtained with *B. mori* silk,¹⁴ the cocoons were boiled for 30 min in distilled water. Fibers ~20 cm long were obtained by pulling gently, and were allowed to dry overnight in air before testing. Small pieces (50 mg) were cut from the degummed cocoon to perform the amino acid analysis. The samples were hydrolyzed overnight in 5 mL of 6 N HCl in a sealed container at 110 °C, and subsequently dried in air. After resuspension in distilled water, aliquots were injected in an automatic amino acid analyzer (Fisons 3A30).

Samples 5 cm long were cut from the degummed material and mounted on a cardboard frame as described elsewhere,^{14, 15} so that the gauge length for tensile tests was $L_0 = 30$ mm. Tensile tests were performed with an Instron 4411 machine to control the strain rate accurately. A balance (Precisa 6100C, resolution ± 10 mg) attached to the lower end of the sample was used instead of a conventional load cell.^{14, 15} The displacement of the crosshead was taken as the deformation of the sample because the compliance of silk is ~1000 times greater than that of any other part of the system.¹⁴ All tensile tests were conducted at a strain rate of 0.0002 s^{-1} .

The experimental arrangement for tests in liquid media is similar to the setup just described except that the frame is made from aluminum foil instead of cardboard. In all cases, the samples were conditioned in the corresponding medium for 2 h prior to testing. No load was applied to the samples during the conditioning period, allowing any contraction of the sample to occur. More details of the experimental configuration can be found elsewhere.¹³ Control samples were tested in air under nominal conditions ($T = 20$ °C; RH = 60 %).

Selected samples were metallized with gold and examined in a scanning electron microscope (JEOL 6300; observation conditions $V = 10$ kV, $I = 0.6$ nA). When necessary, the sample cross sec-

Table I Amino Acid Composition of *Attacus atlas* Silk

Amino Acid	Percentage of Total Number of Amino Acids
Ala	17.98
Asx	4.42
Arg	1.60
Cys	2.74
Glx	3.27
Gly	40.71
His	2.20
Hyp	1.18
Ile	0.11
Leu	0.47
Lys	0.40
Met	1.17
Phe	0.15
Pro	5.23
Ser	8.80
Thr	1.27
Trp	— ^a
Tyr	7.66
Val	0.43

^a Below detection limit.

tion was estimated from micrographs taken at two different positions along the sample, in each case at two different orientations.^{14,15}

RESULTS AND DISCUSSION

Composition of *A. atlas* Silk

The amino acid composition of *A. atlas* silk is shown in Table I. From these data, the disorder ratio for the silk is found to be 26.3%, coinciding with the mean value obtained for other *Saturniidae* silks and for *Nephila madagascarensis* drag line. At the same time, there are significant differences between the composition of *Antheraea* sp. and *A. atlas* silks. In *A. atlas* silk, the majority individual component is glycine instead of alanine, and whereas *Antheraea* shows an alanine content of 37%, the alanine content of *A. atlas* is only 18%. In this respect, the amino acid composition of *A. atlas* silk is close to that of spider major ampullate (drag line) silk;⁷ however, the serine content is higher in *A. atlas* silk.

Tensile Properties of *A. atlas* Silk in Air

Because of the difficulty of measuring the cross section of these samples accurately, and the large

scatter found when comparing the force–displacement (F – d) plots of different samples, it was only possible to obtain approximate absolute values for the mechanical properties. A mean value of $E = 5$ GPa was obtained; this value is larger than the published⁴ value for *Antheraea* silk ($E = 2$ GPa), but lower than the elastic modulus¹⁵ of *B. mori* silk ($E = 16$ GPa).

The strain at breaking in air for *A. atlas* silk ranged between 0.10 and 0.30, with a mean value of $\varepsilon_u = 0.18$. Although this value is lower than the value for *Antheraea* ($\varepsilon_u = 0.35$), it must be emphasized that our mean value for *A. atlas* silk was obtained from 10 tensile tests that show a large scatter. Also, the statistics of breaking are a complex function of flaw size distribution in the material and therefore are likely to be more dependent on process-related factors than on composition.

In view of the poor reproducibility of mechanical tests performed on the *A. atlas* silk, it was necessary to reconsider carefully the basis on which the properties can be compared when assessing the effect of immersion in different environments.

Reproducibility of the Mechanical Properties Obtained from Tensile Tests

It is a well-known fact that samples of a given type of silk may yield very different F – d curves. This scatter can be assigned to differences in the sample cross sections, and possibly to preexisting microstructural flaws.¹⁴ Thus, it should be possible to reduce the variability in measured tensile properties by scaling with respect to precise measurements of the sample cross section. Unfortunately, the small transverse dimensions of the samples, together with a cross-sectional profile that deviates from an ideal circle, generally precludes the desired accuracy of measurement. Although re-scaling F – d plots to display data as stress–strain curves reduces the initial scatter, there is still a large variation in the results.¹⁴

Efforts to overcome this difficulty have long recognized that adjacent samples (i.e., successive samples cut from an original thread) yield similar F – d curves.¹⁰ Thus, the influence of the environment on the mechanical properties of silk should be investigated by comparing F – d curves of samples under the conditions of interest with F – d curves of adjacent samples tested in air (control samples). This methodology has allowed the determination of the influence of water and organic

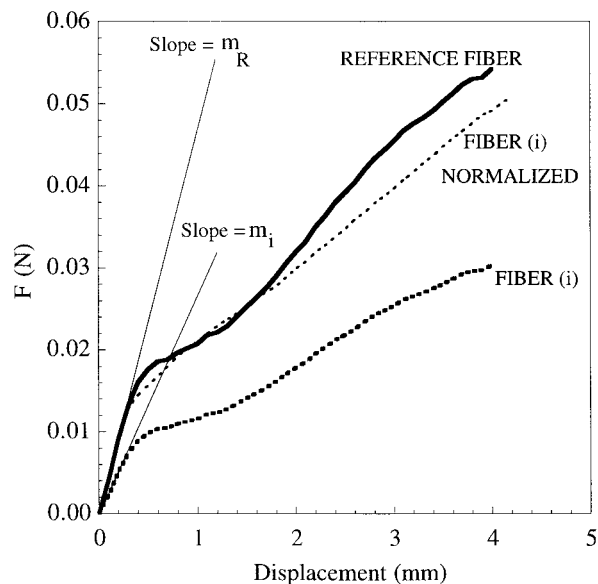


Figure 1 Force–displacement curves of two adjacent *A. atlas* samples (thicker lines), together with the force–displacement curve of the sample labeled *i* (thin line) after normalization relative to the reference sample. (Test conditions: gauge length = 30 mm, strain rate = 0.0002 s^{-1} , RH = 60 % and $T = 20 \text{ }^\circ\text{C}$.)

solvents on the mechanical properties of *B. mori* silk.¹³

We compared F – d curves of adjacent samples to test the success of this methodology on *A. atlas* silk. However, in contrast with previous silks studied, we found that such samples could still exhibit properties differing by a factor of >2 (see Figure 1, thicker lines). In an effort to understand this significant intrinsic variance between adjacent samples, some of the silk was examined by scanning electron microscopy. The main features of the fiber recovered after the degumming process are shown in Figure 2a. Individual filaments $\sim 1 \mu\text{m}$ thick can be recognized clearly (see also detail in Figure 2b), although they are surrounded by a matrix. These micrographs indicate that a standard degumming process is not efficient enough to isolate a monofilament. We are reluctant to degum the material under more aggressive conditions, so all the mechanical property data presented for *A. atlas* silk in this paper have been obtained from samples that are actually bundles consisting of several individual filaments. Interestingly, similar micrographs showing a polyfilament morphology have been found for *Antheraea* species.¹⁶ The polyfilament structure of the incompletely degummed *A. atlas* silk is the most likely cause of the mechanical property

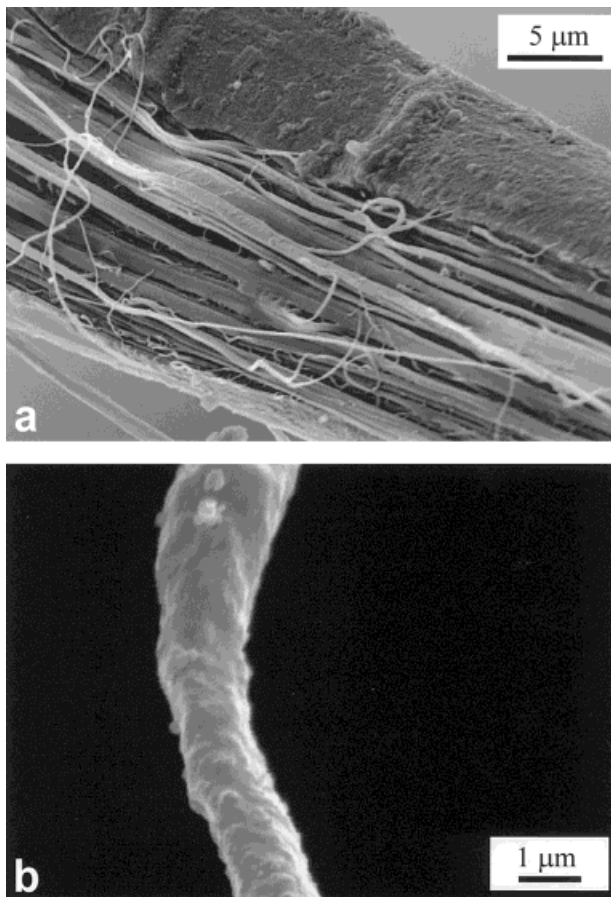


Figure 2 (a) Micrograph of *A. atlas* silk as obtained after degumming the cocoon. The polyfilament structure is readily apparent. (b) Detail of one filament.

differences exhibited by adjacent samples, as well as the large scatter in the cross section along the samples: the number of filaments that constitute the degummed material can change along its length.

Therefore, to minimize the impact of this source of irreproducibility, we sought to devise a protocol that normalizes the tensile test data in a way that is independent of sample cross-sectional area. An obvious requirement is that the normalization parameter should be easily measurable. It can be shown (see Appendix) that the initial slope of the $F-d$ curves can be used to achieve such a normalization of force. The curves $(m_R/m_i)F_i$ versus d should be displayed instead of F_i versus d , where m_R denotes the initial slope of the $F-d$ curve for a sample arbitrarily taken as reference and m_i is the initial slope of the curve for an adjacent sample that is to be compared to the reference.

In Figure 1, the continuous line has been taken as the reference and the normalized F_i versus d corresponding to the adjacent sample is plotted with a thinner line. It is evident that the adjacent samples show similar normalized $F-d$ curves. This normalization procedure was checked with 25 samples obtained from 10 different threads of degummed material, and differences that were always $<15\%$ were found when comparing the normalized data from adjacent samples. The fact that normalization does not eliminate all of the differences between test results may reflect the existence of preexisting flaws in silk.¹⁴

A useful corollary can be deduced from these considerations: adjacent samples with the same value of m (i.e., $m_R = m_i$) yield similar $F-d$ curves. Therefore, provided that the test and adjacent reference samples do yield the same value of m , we can dispense with the need to actually perform the normalization. Data can then be compared directly in the form of the as-recorded $F-d$ curves, facilitating presentation of results. In practice, such coincident values of m occur rarely, so we have adopted an arbitrary criterion of only presenting data for cases where the test and reference values of m differ by $<5\%$.

When samples were prepared for testing in water or ethanol, they were first tested within their elastic regime in air. The initial slope of their $F-d$ response was compared with that obtained by testing the adjacent control sample in air. If the two values differed by $>5\%$, a new pair of adjacent test and control samples was considered.

Implicitly, the validity of this procedure requires the existence of a true elastic region in the $F-d$ curve, so that a sample can be loaded and unloaded in air without altering the mechanical properties irreversibly before it is submerged in the liquid medium of interest. Unloading-reloading tests have been performed to confirm the existence of an initial elastic response. The $F-d$ curve of a tensile test with three unloading-reloading steps is shown in Figure 3. It is evident that the initial unloading-reloading step does not alter the mechanical properties of the fiber, thus defining a *true* elastic region. The data in Figure 3 also demonstrate that there is a clear limit beyond which unloading-reloading steps result in irreversible changes to this material. Similar behavior has been described previously for *B. mori* silk.¹⁴

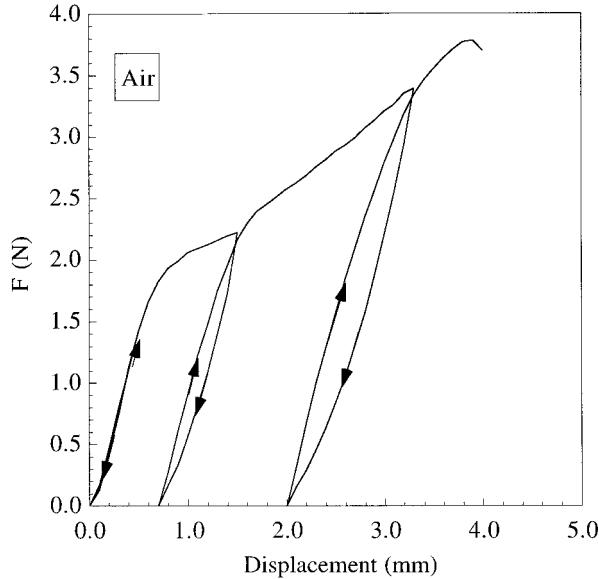


Figure 3 Tensile test in air with three unloading–reloading steps. (Test conditions: gauge length = 30 mm, strain rate = 0.0002 s^{-1} , RH = 60 %, and $T = 20\text{ }^{\circ}\text{C}$.)

Mechanical Properties in Liquid Media

Two solvents have been used in this study. Water was chosen because it is responsible for the supercontraction of spider silk and its effect on *B. mori* silk has been characterized as well.¹³ Ethanol also has a supercontracting effect on spider drag line silk¹² (although this is more modest than the effect of water), and it exerts a desiccating effect on *B. mori* silk.¹³

Because supercontraction is inhibited in stressed samples, the Instron crosshead was lowered 5 mm from the initial position ($F = 0\text{ N}$ in air) before the corresponding solvent was introduced. This procedure ensured that no force was exerted on the sample while it was being conditioned in the solvent. After starting tensile tests in the liquid media, the position of the crosshead at which load was first exerted on the sample was recorded and compared with the initial position of the crosshead ($F = 0\text{ N}$ in air). The difference between these positions was used to measure any supercontraction of the sample. Both crosshead positions coincided under all the conditions studied, so supercontraction does not occur in either of the liquid media.

Examples of the tests performed in air, water, and ethanol are shown in Figures 4, 5, and 6, respectively. The F – d curves of three adjacent samples tested in air (control sample), water, and ethanol are compared in Figure 7. There is a large

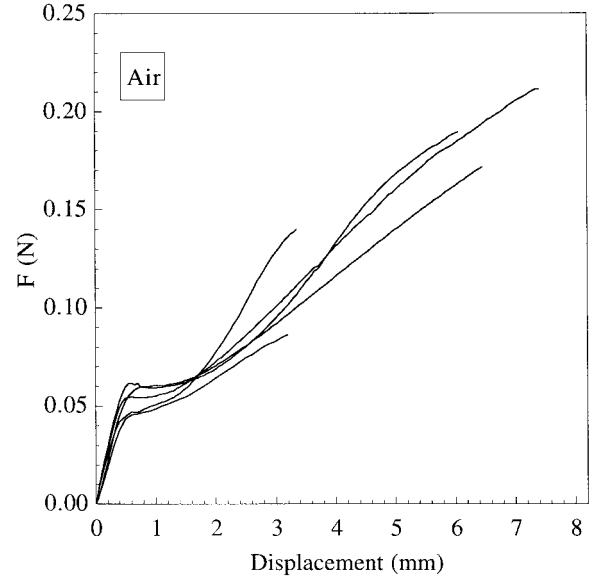


Figure 4 Comparison of the force–displacement curves of five samples tested in air. (Test conditions: gauge length = 30 mm, strain rate = 0.0002 s^{-1} , RH = 60 %, and $T = 20\text{ }^{\circ}\text{C}$.)

decrease in the initial slope in water compared with the control sample, but for strains ≥ 0.07 ($d \approx 2.1\text{ mm}$), both curves run almost parallel. In contrast, little change in the initial slope is observed for the sample submerged in ethanol, but

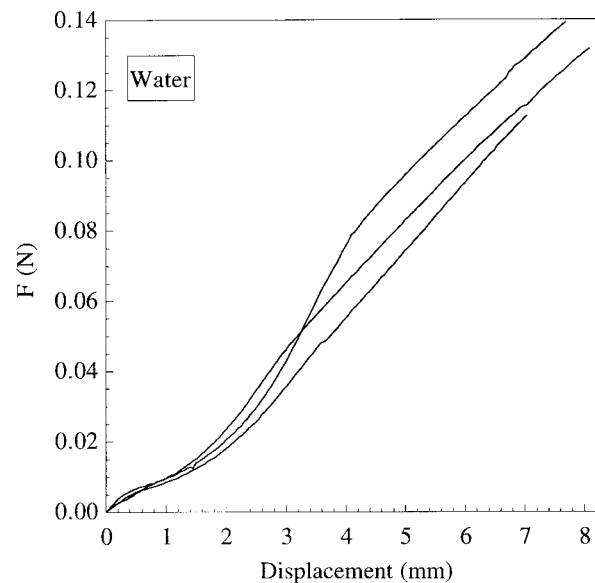


Figure 5 Comparison of the force–displacement curves of three samples tested in water. (Test conditions: gauge length = 30 mm, strain rate = 0.0002 s^{-1} , and $T = 20\text{ }^{\circ}\text{C}$.)

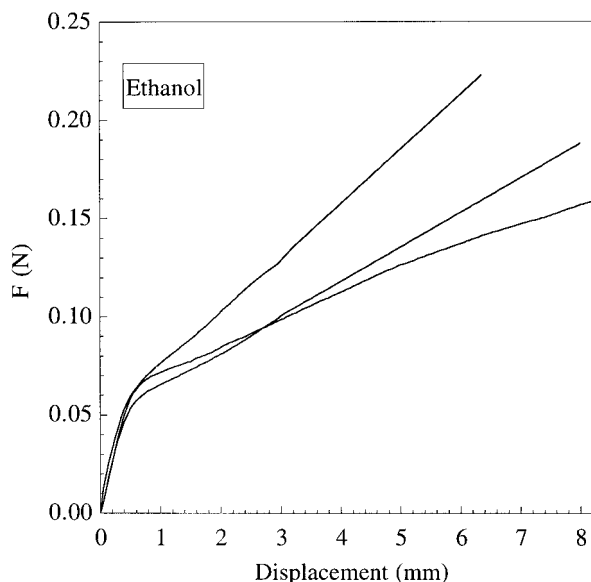


Figure 6 Comparison of the force–displacement curves of three samples tested in ethanol. (Test conditions: gauge length = 30 mm, strain rate = 0.0002 s^{-1} , and $T = 20 \text{ }^\circ\text{C}$.)

the curve differs from the control beyond the elastic region whereupon it can be approximated by a straight line.

Ten tests were performed in each medium, yielding very similar results (because the results superimpose so well, only a subset is displayed in Figures 4, 5, and 6 for clarity). Mean values of the tensile parameters are shown in Table II. Following the discussion just presented, F – d curves of samples submerged in each medium were compared with F – d curves of adjacent control samples tested in air; therefore, relative values of the initial slope ($m_{\text{medium}}/m_{\text{air}}$), stress at the proportional limit ($\sigma_{p, \text{medium}}/\sigma_{p, \text{air}}$), and tensile strength ($\sigma_{u, \text{medium}}/\sigma_{u, \text{air}}$) are presented. The absolute values of ε_p and ε_u in air represent the average of 10 tests.

The characterization of *A. atlas* silk submerged in water and ethanol included unloading–reloading tests. Tests in water and ethanol are shown in Figures 8 and 9, respectively. The existence of a true elastic regime, where the samples can be unloaded and reloaded without undergoing any permanent deformation, is confirmed in both cases. Unloading–reloading steps in both media can be approximated by straight lines whose slopes are similar to the initial slope of the F – d curve. Beyond the true elastic regime for samples tested in ethanol, the final point of reloading does not coincide with the initial point of unloading;

this behavior was found in the three different samples subjected to unloading–reloading steps. Close examination of Figure 3 reveals that the behavior in air is similar (the difference between the position of the starting point of unloading and the final point of reloading is approximately the same as for the tests in ethanol, but the effect is less apparent in Figure 3 because the vertical scale is more compressed than in Figure 9). In contrast, both points coincide when the test is performed in water (Figure 8).

From the data just presented, it is apparent that many tensile properties of *A. atlas* silk in both solvents are qualitatively similar to those observed previously for *B. mori*,¹³ including (a) absence of supercontraction, (b) significant reduction of E after immersion in water, and (c) (slight) increase of E after immersion in ethanol. Observations (a) and (c) contrast with the behavior reported for spider drag line silk.¹² It has been argued that the dissimilar behavior of *B. mori* silk and spider drag line reflects profound differences in the basic microstructural arrangements of both materials. Supercontraction and the elastomeric behavior of spider silk in water are prompted by large changes in the conformation of the protein, so that they can be considered as *entropic* effects.¹¹ On the other hand, when *B. mori* silk is immersed in water, hydrogen bonds between protein chain segments are substituted by

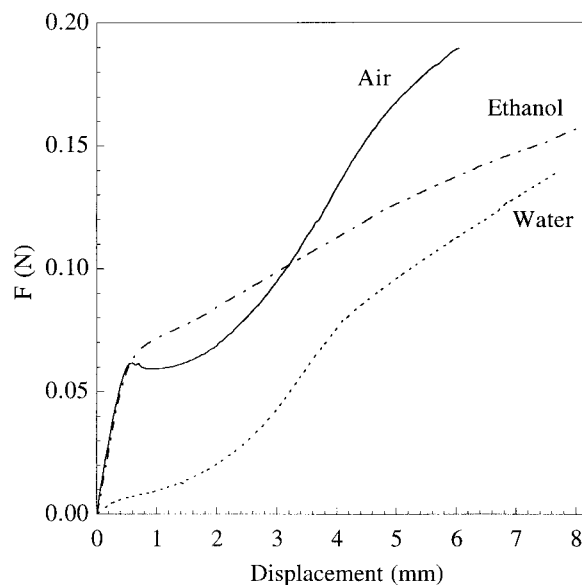


Figure 7 Comparison of the force–displacement curves of three adjacent samples: control sample (in air), ethanol, and water. (Test conditions: gauge length = 30 mm, strain rate = 0.0002 s^{-1} , and $T = 20 \text{ }^\circ\text{C}$.)

Table II Mean Tensile Properties of *Attacus atlas* Silk in Different Media^a

Medium	$m_{\text{medium}}/m_{\text{air}}$ ($\equiv E_{\text{medium}}/E_{\text{air}}$)	$\sigma_{p,\text{medium}}/\sigma_{p,\text{air}}$	ϵ_p	$\sigma_{u,\text{medium}}/\sigma_{u,\text{air}}$	ϵ_u
Water	0.13 ± 0.01	0.12 ± 0.01	0.010 ± 0.001	1.0 ± 0.1	0.29 ± 0.02
Ethanol	1.06 ± 0.03	1.05 ± 0.08	0.010 ± 0.001	1.03 ± 0.07	0.23 ± 0.02
Air	1	1	0.011 ± 0.001	1	0.18 ± 0.01

^a m = initial slope of force-displacement (F-d) curve; E = elastic modulus; σ_p = stress at proportional limit; ϵ_p = strain at proportional limit; σ_u = tensile strength; ϵ_u = strain at breaking; the proportional limit is defined as the point where the F-d curve intersects a straight line that passes through the origin and has a slope equal to 95% of the initial slope of the curve.

water—protein hydrogen bonds, so the decrease in tensile properties can be considered as an *enthalpic* effect.¹³ Because the tensile properties of *A. atlas* silk parallel the behavior of *B. mori* silk, the effect of water can be similarly attributed to the substitution of interprotein hydrogen bonds by water—protein hydrogen bonds, with no significant change in the conformation of the protein. Likewise, the qualitatively comparable effect of ethanol on the two silks suggests that the interpretation of the behavior of *B. mori* silk in this solvent¹³ is also applicable to *A. atlas* silk: ethanol desiccates the material, increasing the number of interprotein hydrogen bonds.

Three further aspects of *A. atlas* silk behavior can be understood in the context of these effects of water and ethanol. First, the disruptive action of water will enhance microstructural mobility and so

may explain why, beyond the true elastic regime, the unloading and reloading curves of *A. atlas* silk in water merge rather than cross at the final point of reloading (Figure 8). Second, the smaller modulus increase for *A. atlas* silk ($E_{\text{ethanol}}/E_{\text{air}} = 1.06 \pm 0.03$) compared with *B. mori* silk ($E_{\text{ethanol}}/E_{\text{air}} = 1.21 \pm 0.04$) in ethanol may be attributable to the former silk having a lower inherent moisture content. Third, the larger modulus decrease for *A. atlas* silk ($E_{\text{ethanol}}/E_{\text{air}} = 0.13$) compared with *B. mori* silk ($E_{\text{ethanol}}/E_{\text{air}} = 0.27$) in water is consistent with the previous point.

We have not attempted to compare the tensile strength or the strain at breaking of *A. atlas* silk with that of *B. mori* silk in the different environments or to explain the effect of the different environments on these characteristics for either silk. The fracture behavior of silk follows the fail-

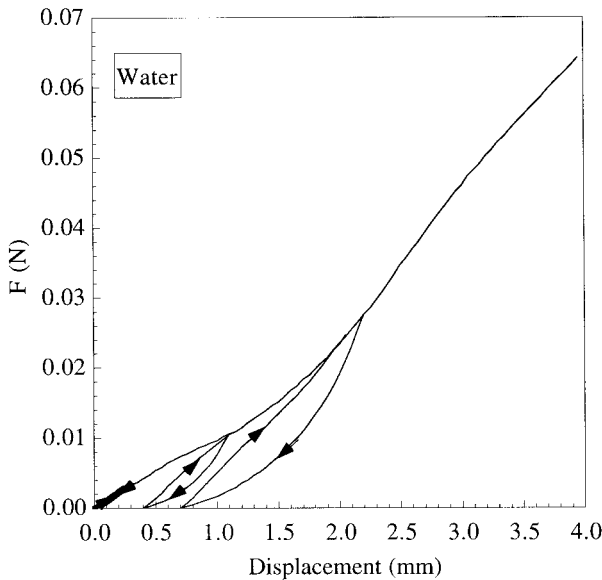


Figure 8 Tensile test in water with three unloading–reloading steps. (Test conditions: gauge length = 30 mm, strain rate = 0.0002 s^{-1} .)

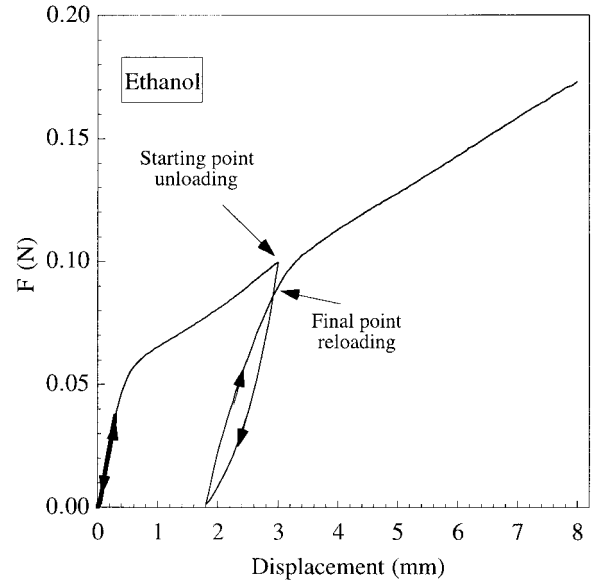


Figure 9 Tensile test in ethanol with three unloading–reloading steps. (Test conditions: gauge length = 30 mm, strain rate = 0.0002 s^{-1} .)

ure statistics of a brittle material,¹⁴ implying that intrinsic flaws may play a controlling role. Under these circumstances, the sample volume becomes an important factor and it would not be appropriate to compare results from specimens that consist of a variable number of flawed parallel monofilaments.

Finally, we note that the value of the strain at the proportional limit is not sensitive to chemical environment; this is also true for *B. mori* silk. Indeed the value is closely similar for both silks. This observation suggests that the relative amounts of crystalline and amorphous material, and their distribution and connectivity in the microstructure, combine to achieve the same reinforcement in both materials. Although we might expect less crystalline reinforcement in *A. atlas* silk — the disorder index is twice that for *B. mori* silk — it is not just the size but also the number and effectiveness of microstructural pinning centers that matter here. These parameters will limit the macroscopic geometrical change that can be accommodated elastically, and they are not altered by the chemical environment. What the environment does alter is microstructural mobility, thereby affecting the stress needed to achieve the limiting elastic shape change and the stress needed to propagate subsequent permanent deformation.

CONCLUSIONS

The amino acid composition of *A. atlas* silk was similar to that published for other silks from the *Saturniidae* family and spiders (i.e., *Nephila madagascarensis* drag line), but different from that of *B. mori* silk, when the materials were compared in terms of their disorder ratio. The tensile properties of *A. atlas* silk in air, water, and ethanol were measured and compared with previous results from *B. mori* and spider drag line silks. Variability in the F - d plots collected from a given silk under a given set of conditions can be reduced significantly by normalizing data with respect to the initial slope of an arbitrarily chosen reference plot.

Despite its compositional similarities to spider dragline, *A. atlas* silk exhibits no significant contraction when submerged in either water or ethanol. The effect of both fluids on the tensile properties of *A. atlas* silk is qualitatively similar to their effect on *B. mori* silk. Immersion in water greatly reduces the elastic modulus, whereas im-

mersion in ethanol leads to a (slight) increase in modulus, relative to control samples characterized in air. Collectively, the results for *A. atlas* silk are consistent with water having a disruptive effect on protein—protein hydrogen bonds, and ethanol having a desiccating effect.

The results demonstrate that silks with different amino acid compositions (i.e., *A. atlas* and *B. mori*) may exhibit similar mechanical properties and, conversely, silks with similar amino acid compositions (i.e., *A. atlas* and *Nephila* sp.) may exhibit different mechanical properties. Because mechanical properties depend on microstructure, it is evident that invertebrates have evolved to produce microstructural diversity that is not constrained by primary composition. In other words, primary composition is not a simple indicator of function in silks, and the search for correlations between microstructure and properties remains a worthwhile, albeit formidable goal.

The authors thank J. I. Pardo de Santayana and the Zoological Park of Santillana del Mar (Santander, Spain) for kindly providing the *Attacus atlas* cocoons. They are also grateful to Ms. P. Sanz (Centro de Diagnóstico de Enfermedades Moleculares, Centro de Biología Molecular “Severo Ochoa”, Spain) for performing the amino acid analysis. Partial support for this work was received from the Ministerio de Educación y Cultura (Spain) and the British Council through an Acción Integrada.

APPENDIX

Details of the Normalization Method

Consider two fibers (i denoting a fiber of interest and R denoting a reference fiber) that exhibit the same stress–strain characteristics but have different cross sections. Implicitly, they exhibit the same intrinsic properties. If they support the same stress, $\sigma_R = \sigma_i$, then by definition:

$$\frac{F_R}{A_R} = \frac{F_i}{A_i} \quad (\text{A1})$$

or

$$F_R = \frac{A_R}{A_i} F_i \quad (\text{A2})$$

where F represents force and A represents area. This equation defines our normalization procedure.

Thus, both the reference force–displacement (F_R – d) curve and the normalized F_i – d curve should be similar. In principle, the use of eq. A2 may not seem to represent any advantage compared with the use of the usual eq. A1. However, the use of eq. A1 requires the direct measurement of both cross sections, whereas the use of eq. A2 requires only the *ratio* of both the cross-sectional areas to be determined.

This ratio can be obtained by considering the initial elastic region of the F – d curve, which satisfies the equation

$$F = m \cdot d \quad (\text{A3})$$

where F represents force, d represents displacement, and m is the slope of the plot. But,

$$F = \sigma \cdot A_0,$$

where σ is the corresponding stress, A_0 is the cross section, and $\varepsilon = d/l_0$, with ε representing strain and l_0 representing reference length. Therefore eq. A3 can be written as

$$\sigma \cdot A_0 = m \cdot \varepsilon \cdot l_0 \quad (\text{A4})$$

Substituting stress from $\sigma = E \cdot \varepsilon$ and simplifying, an expression for m is obtained:

$$m = \frac{A_0 E}{l_0} \quad (\text{A5})$$

where E is the elastic modulus.

If two samples have the same elastic modulus and the same reference length, the quotient m_R/m_i is therefore equal to

$$\frac{m_R}{m_i} = \frac{A_R}{A_i} \quad (\text{A6})$$

It follows that the ratio of the cross-sectional areas can be determined from the initial slopes of the F – d curves of both samples. Substituting in eq. A2,

$$F_R = \frac{m_R}{m_i} F_i \quad (\text{A7})$$

Thus, the normalized force $m_R/m_i \cdot F_i$ will coincide with the force of the reference sample if both materials have the same stress–strain curve.

REFERENCES

1. Kaplan, D.; Adams, W.W.; Farmer, B.; Viney, C. In *Silk Polymers*. Materials Science and Biotechnology; ACS Symposium Series 544; American Chemical Society: Washington, DC, 1994; pp 2–16.
2. *Int J Biol Macromol* 1999, 24, 81–306 (special issue on silks).
3. Zemlin, J.C. Technical Report 69-29-CM (AD 684333), (1968), U.S. Army Natick Laboratories, Natick, MA.
4. Kaplan, D.L.; Lombardi, S.J.; Muller, W.S.; Fossey, S.A. In *Biomaterials. Novel Materials from Biological Sources*; Byrom, D., Ed.; Stockton Press, New York, 1991; pp 3–53.
5. Lucas, F.; Shaw, J.T.B.; Smith, S.G. *J Textile Inst*, 1955, 46, 440–452.
6. Lombardi, S.J.; Kaplan, D.L. *J Arachnol* 1990, 18, 297–306.
7. Work, R.W.; Young, C.T. *J Arachnol* 1987, 15, 65–80.
8. Marsh, R.E.; Corey, R.B.; Pauling, L. *Biochim Biophys Acta* 1955, 16, 1–34.
9. Thiel, B.L.; Viney, C. *J Microsc* 1997, 185, 179–187.
10. Work, R.W. *Textile Res J* 1977, 47, 650–662.
11. Gosline, J.; Denny, M.V.; DeMont, M.E. *Nature* 1984, 309, 551–552.
12. Shao, Z.; Vollrath, F. *Polymer* 1999, 40, 1799–1806.
13. Pérez-Rigueiro, J.; Viney, C.; LLorca, J.; Elices, M. *Polymer* 2000, 41, 8433–8439.
14. Pérez-Rigueiro, J.; Viney, C.; LLorca, J.; Elices, M. *J Appl Polym Sci* 1998, 70, 2439–2447.
15. Pérez-Rigueiro, J.; Viney, C.; LLorca, J.; Elices, M. *J Appl Polym Sci* 2000, 75, 1270–1277.
16. Bhat, N.V.; Nadiger, G.S. *Textile Res J* 1978, 48, 685–691.